ELSEVIER

Journal of Hazardous Materials B80 (2000) 119–133

Journal of Hazardous Materials

www.elsevier.nl/locate/jhazmat

Sulfation and attrition of calcium sorbent in a bubbling fluidized bed

Chen-Yeon Chu, Kuang-Wei Hsueh, Shyh-Jye Hwang*

Department of Chemical Engineering, National Tsing Hua University, 101 Kuang Fu Road, Hsinchu 30043, Taiwan, ROC

Received 21 March 2000; received in revised form 30 June 2000; accepted 3 July 2000

Abstract

A bubbling fluidized bed reactor was used as a desulfurization apparatus in this study. The height of the bed was 2.5 m, and the inner diameter was 9 cm. The bed materials were calcium sorbent and silica sand. The effects of the operating parameters of the flue gas desulfurization including relative humidity, temperature, superficial gas velocity, and the particle size of calcium sorbent on SO_2 removal efficiency and calcium sorbent conversion and attrition rate in the fluidized bed were investigated. It was found that the temperature effect in our system was negligible from 40 to 65°C. A higher relative humidity had a higher calcium conversion and a higher sulfur dioxide removal efficiency. Moreover, a smaller particle size of calcium sorbent had a lower calcium conversion in the cyclone but a higher sulfur dioxide removal efficiency. A lower superficial gas velocity resulted in a higher sulfur dioxide removal efficiency and a higher calcium conversion, thus, the total volume of the flue gas treated was maximum near the minimum fluidization velocity. Finally, an attrition rate model proposed in this study could predict the elutriation rate satisfactorily.

Keywords: SO_2 removal efficiency; Calcium conversion; Bubbling fluidized bed; Attrition; Elutriation

1. Introduction

SO_2 is one of the major air pollutants from coal-fired electric power plants and waste incinerators. A variety of processes are available for SO_2 control. A wet process using calcium carbonate as the absorbent is most commonly adopted in commercial plants. The wet process has a high SO_2 removal efficiency but uses a large amount of water and the resultant wastewater has to be treated. Semi-dry FGD scrubber, also known as spray dryer, has been widely accepted as an effective practice to remove SO_2 from flue gas generated by

* Corresponding author. Tel.: +886-3-5723221; fax: +886-3-5715408.
E-mail address: sjhwang@che.nthu.edu.tw (S.-J. Hwang).

0304-3894/00/$ – see front matter
PII: S0304-3894(00)00290-9

the combustion of low-sulfur coal and municipal solid waste. The advantages of the spray dryer compared to the wet scrubber include lower capital and operating cost, reduction in corrosion and scaling problems, and elimination of wet-sludge by-product. A dry process using calcium hydroxide as the absorbent has been used commercially, but it is not as common as the wet process. In the dry process, calcium hydroxide powder is injected into the duct. The SO_2 removal efficiency of the duct injection dry process, however, is not high. Moreover, a large fraction of calcium hydroxide remains unreacted.

In this study, a bubbling fluidized bed was used as a desulfurization apparatus. Fluidization is the operation by which solid particles are transformed into a fluid-like state through suspension in a gas [1]. One of the special features of the fluidized bed is high attrition of the particles in the bed, which would remove the product layer of sulfation and increase the utilization of the calcium sorbent.

Reports on attrition in the fluidized bed were numerous (e.g. [2–4]). However, investigation of simultaneous sulfation and attrition in the fluidized are limited. Bernedetto and Salatino [5] studied the attrition of limestone during calcination and sulfation in a fluidized bed reactor. They reported that the attrition during the sulfation of precalcined limestone was dominated by conversion of lime into sulfate. They proposed a model which took into account the parallel occurrences of abrasion and gas–solid reaction. However, their model was very complex and difficult to use. The present work investigates the attrition rate and its effect on the sulfation of the sorbent. By considering the parallel occurrences of abrasion and gas–solid reaction, we also propose a model to predict the attrition rate in the fluidized bed. The model, however, is simple and easy to use.

2. Experimental

A schematic diagram of the experimental apparatus is shown in Fig. 1. The fluidized bed was made of quartz, and its inner diameter and height were 9 cm and 2.5 m, respectively. The distributor at the bottom of the bed was a stainless-steel perforated plate with 0.2 cm holes on an equilateral triangle pitch, and the distance between holes was 0.3 cm. A sheet of steel screen (mesh #400) covered the distributor to prevent the bed materials from falling into the windbox.

The bed materials were calcium sorbent and silica sand. The chemical and physical properties of the calcium sorbent measured by atomic absorption spectrometer (AAS) (Varian, SpectrAA-30), thermogravimetric analyzer (TGA) (Dupont 2100, General V4.1c) and accelerated surface area porosimetry (ASAP) (Micromeritics Instrument Corporation, ASAP 2000 V2.05) are shown in Table 1. The average diameter of the silica sand, d_{ps}, was 460 μm, while those of the calcium sorbent, d_{pc}, were 254, 324, 385, and 460 μm. The densities of the calcium sorbent and silica sand were 2300 and 2630 kg/m^3, respectively. The weights of the calcium sorbent and silica sand in the bed were 500 and 1500 g, respectively. Thus, the static bed height was 25 cm. A cyclone and a bag filter collected all the fines carried over, and the fines were weighed to obtain the attrition rate. Note that we assumed the elutriation rate was the same as the attrition rate because the superficial gas velocity used in the experiments was always less than the terminal velocity of the particles. This method was similar to that used by Kono [6] or Ray et al. [2]. TGA was used to measure the con-

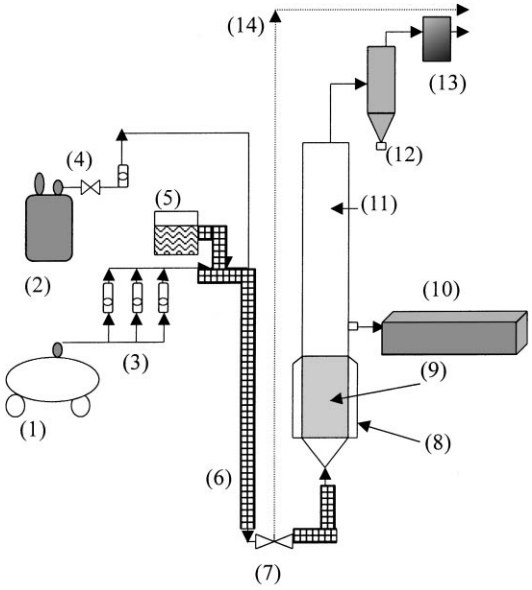

(1) Air compressor (2) SO_2 cylinder (3) Rotameter (4) Pressure regulator (5) Humidification system (6) Preheating tape (7) Three-way valve (8) Oil bath (9) Fluidized bed (10) SO_2 analyzer (11) Freeboard (12) Cyclone (13) Bag filter (14) By pass

Fig. 1. Schematic diagram of the experimental apparatus.

version of the calcium sorbent in the bed and the cyclone. Before each measurement we analyzed the particles by an X-ray powder diffraction (XRD) (Scintac Inc., USA) to ensure the composition of the product was $CaSO_3 \cdot (1/2)H_2O$. We could then calculate the calcium conversion by the TGA diagram.

Synthetic flue gas was made by mixing compressed air from an air compressor and SO_2 gas from an SO_2 cylinder. Rotameters were used to measure the gas flow rate, while preheating tapes and an oil bath around the fluidized bed were utilized to control the temperatures of the gas and the bed, respectively. In addition, the humidity of the flue gas was adjusted by a

Table 1
Chemical and physical properties of the calcium sorbent

Chemical composition	Weight (%)	Physical characteristics		
		Particle range (μm)	Average particle size (μm)	BET surface area (m^2/g)
CaO	62.46	500–420	460	3.26
$Ca(OH)_2$	27.00	420–350	385	4.77
$CaCO_3$	4.56	350–297	324	5.59
MgO	3.42	297–210	254	6.41
Others	2.56			

humidification system. The flue gas entered the bottom of the fluidized bed through the distributor. The inlet and outlet concentrations of SO_2 were measured by NDUV (ANARAD, AR-400). The removal efficiency (R.E.%) of SO_2 was defined as

$$\text{R.E. (\%)} = \frac{C_0 - C}{C_0} \times 100\,(\%) \tag{1}$$

where C_0 and C are inlet and outlet concentrations of SO_2 (ppm), respectively.

In this study, the effects of the bed temperature, relative humidity, particle size, and superficial gas velocity on the removal efficiency of SO_2 and the calcium conversion were investigated.

3. Results and discussion

3.1. Effect of the bed temperature

Typical experimental results for the effect of the bed temperature on the sulfur dioxide removal efficiency are shown in Fig. 2. We found that the sulfur dioxide removal efficiency was not affected significantly by the bed temperature ranging from 40 to 65°C. This was similar to that observed by Ho and Shih [7] in a fixed bed. We also found from Fig. 2 that the sulfation could be divided into three stages. At the first stage, all of the inlet

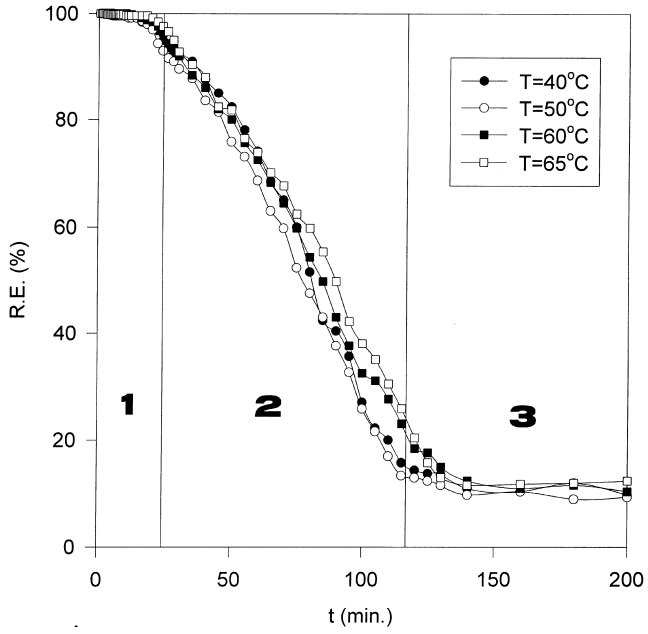

Fig. 2. Removal efficiency of SO_2 at different bed temperatures ($d_{ps} = 460\,\mu m$, $d_{pc} = 254\,\mu m$, $C_0 = 500$ ppm, $U_0 = 20$ cm/s, $W_{s0} = 1500$ g, $W_{c0} = 500$ g and R.H. = 60%).

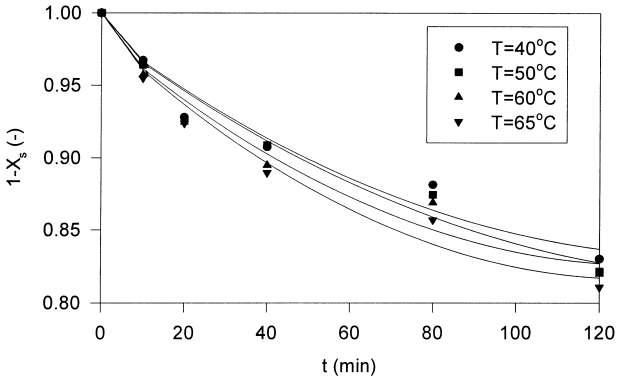

Fig. 3. Conversion of sorbent in the cyclone at different bed temperatures ($d_{ps} = 460\,\mu m$, $d_{pc} = 254\,\mu m$, $C_0 = 500\,ppm$, $U_0 = 20\,cm/s$, $W_{s0} = 1500\,g$, $W_{c0} = 500\,g$ and R.H. = 60%).

sulfur dioxide was absorbed and reacted at the surface of the calcium sorbent. As a result, the removal efficiency was close to 100%. At the second stage, a low porosity product layer ($CaSO_3{\cdot}(1/2)H_2O$) formed gradually at the surface of the sorbent. Consequently, the diffusion resistance of SO_2 from the emulsion phase to the inner unreacted calcium sorbent gradually increased. Thus, the removal efficiency kept decreasing. At the third stage, the removal efficiency of SO_2 was quite low due to the formation of a thick product layer on the sorbent surface. Similar phenomena were observed when the fluidized bed was operated under different relative humidities, average particle diameters and superficial gas velocities.

The effects of the bed temperature on the conversion of the calcium sorbent in the cyclone and the sorbent attrition rate were similar to that on the sulfur dioxide removal efficiency. These are shown in Figs. 3 and 4. Note that the fine particles collected in the cyclone were the solid particles elutriated from the fluidized bed. Fig. 5 shows the conversion of the fine particles in the cyclone, X_s, versus that of the particles in the bed, X_b. It is seen in this figure

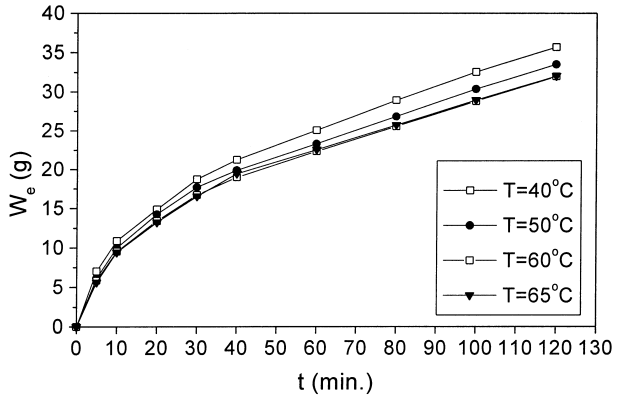

Fig. 4. Cumulative weight of solid elutriated at different bed temperatures ($d_{ps} = 460\,\mu m$, $d_{pc} = 254\,\mu m$, $C_0 = 500\,ppm$, $U_0 = 20\,cm/s$, $W_{s0} = 1500\,g$, $W_{c0} = 500\,g$ and R.H. = 60%).

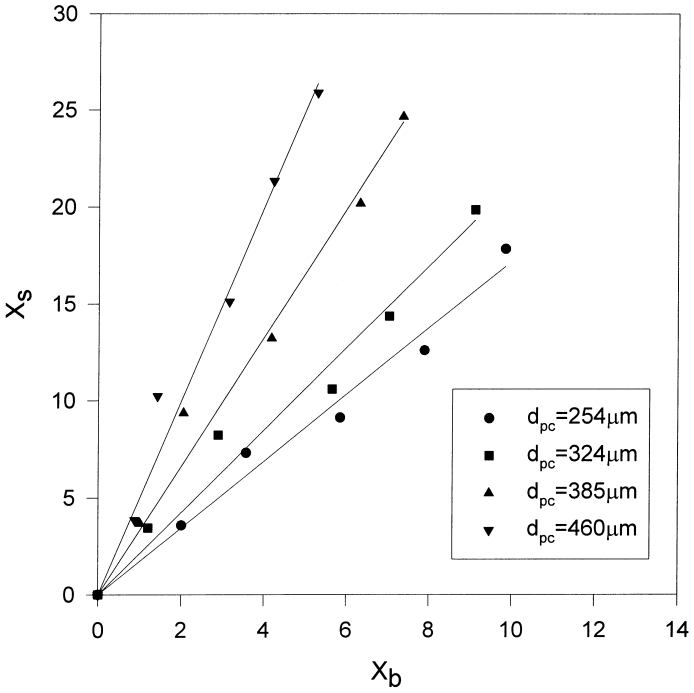

Fig. 5. Conversion of sorbent in the cyclone vs. conversion of the sorbent in the bed at different average particle diameters ($d_{ps} = 460\,\mu m$, $C_0 = 500\,ppm$, $U_0 = 20\,cm/s$, $W_{s0} = 1500\,g$, $W_{c0} = 500\,g$, R.H. = 60% and $T = 50^{\circ}C$).

that the degree of conversion of the fine particles in the cyclone increases with increasing conversion of the particles in the fluidized bed. As a result, it could represent the utilization of the sorbent. Moreover, as shown in Fig. 4, the attrition was fast initially and then decreased slowly with time. These results were consistent with Colakyan and Levenspiel [8] and Cook et al. [9].

3.2. Effect of the relative humidity

The sulfur dioxide removal efficiency and the calcium conversion at different relative humidities are shown in Figs. 6 and 7. It is seen in these figures that the sulfur dioxide removal efficiency and the sorbent conversion increased with an increase in the relative humidity. A higher relative humidity of the flue gas resulted in a thicker liquid film around the sorbent surface. As a result, more SO_2 was absorbed and reacted at the sorbent surface. Note that these results were consistent with those reported by Klingspor et al. [10] and Jorgensen and Chang [11].

Fig. 8 shows the cumulative weight of the solids elutriated at different relative humidities. The attrition rate decreases with increasing relative humidity. This was due to the fact that a higher relative humidity has a higher sorbent conversion. As a consequence, the particles hardened due to the molecular cramming reported by Bernedetto and Salatino

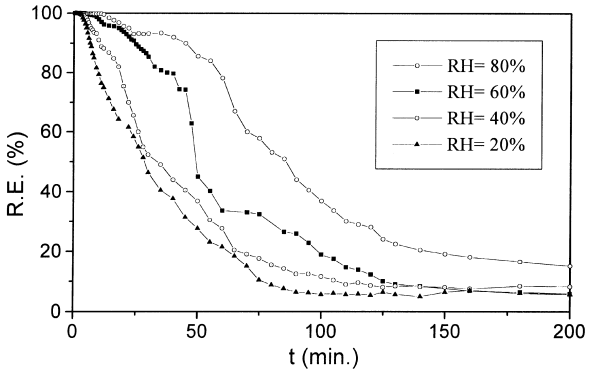

Fig. 6. Removal efficiency of SO_2 at different relative humidities ($d_{ps} = 460\,\mu m$, $d_{pc} = 385\,\mu m$, $C_0 = 500\,ppm$, $U_0 = 20\,cm/s$, $W_{s0} = 1500\,g$, $W_{c0} = 500\,g$ and $T = 50^{\circ}C$).

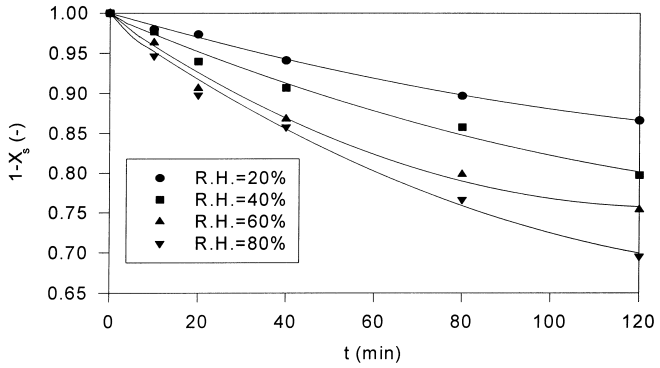

Fig. 7. Conversion of sorbent in the cyclone at different relative humidities ($d_{ps} = 460\,\mu m$, $d_{pc} = 385\,\mu m$, $C_0 = 500\,ppm$, $U_0 = 20\,cm/s$, $W_{s0} = 1500\,g$, $W_{c0} = 500\,g$ and $T = 50^{\circ}C$).

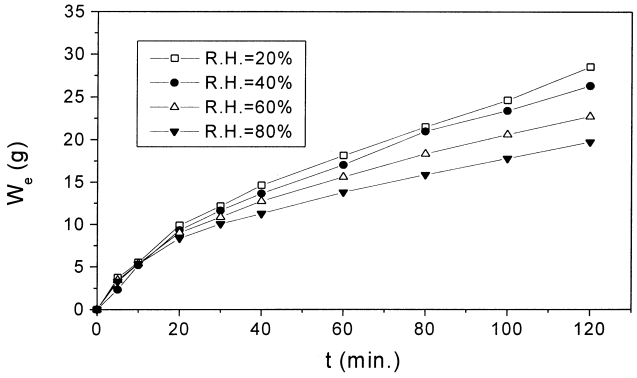

Fig. 8. Cumulative weight of solid elutriated at different relative humidities ($d_{ps} = 460\,\mu m$, $d_{pc} = 385\,\mu m$, $C_0 = 500\,ppm$, $U_0 = 20\,cm/s$, $W_{s0} = 1500\,g$, $W_{c0} = 500\,g$ and $T = 50^{\circ}C$).

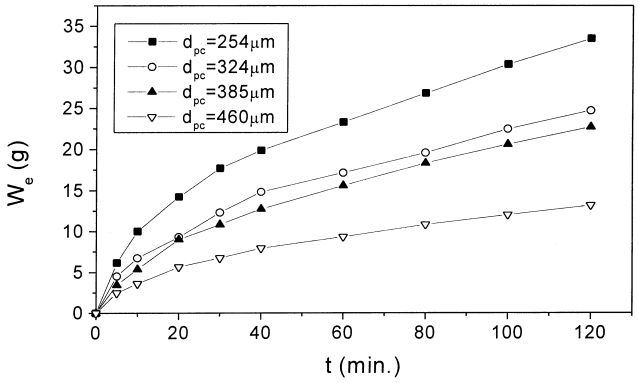

Fig. 9. Cumulative weight of solid elutriated at different average particle diameters ($d_{ps} = 460\ \mu m$, $C_0 = 500$ ppm, $U_0 = 20$ cm/s, $W_{s0} = 1500$ g, $W_{c0} = 500$ g, R.H. = 60% and $T = 50^{\circ}C$).

[5]. They proposed that "partly sulfated grains that still contain unreacted calcium oxide become increasingly crammed against each other and are, as a consequence, less easily attrited as sulfation proceeds". Thus, the attrition rate decreased as the relative humidity was increased. Furthermore, the calcium sorbent particles were dispersed uniformly by the violently moving silica sand particles in the bed. As a result, particle agglomeration at higher humidities was not observed in our study.

3.3. Effect of the particle size

Mixtures of silica sand (460 μm) and four different average diameters of the sorbent particles (254, 324, 385, 460 μm) were used as the bed materials. The weight ratio of the sand and the sorbent was 3:1. Fig. 9 shows the cumulative weight of the solid elutriated at different average particle diameters. As shown in this figure, the attrition decreased with increasing particle diameter. This is due to the fact that the total external particle surface exposed to attrition by abrasion is smaller when the particle diameter is larger [2]. The effect of the particle size on the removal efficiency of SO_2 is shown in Fig. 10. The removal efficiency decreased as the particle size was increased due to decreasing particle surface area for the sulfation reaction.

However, as shown in Fig. 11, the conversion of the sorbent in the cyclone increased with increasing particle size. Since the attrition of smaller particles was higher (Fig. 9), a lot of unreacted or slightly reacted fine particles were elutriated from the bed to the cyclone. Consequently, the sorbent conversion increased as the particle size was increased. It should be noted in Figs. 9 and 11 that the attrition rate decreased with increasing sorbent conversion.

3.4. Effect of the superficial gas velocity

Fig. 12 shows the cumulative weight of the elutriated solid at four different superficial gas velocities. The attrition rate increased as the superficial gas velocity was increased. This was similar to that reported by Merrick and Highley [12] and Lin et al. [13].

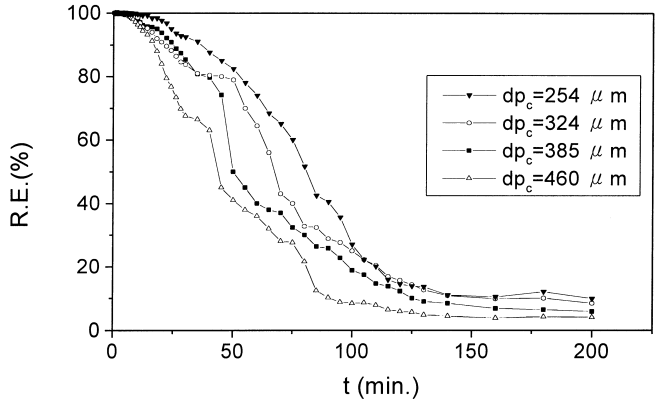

Fig. 10. Removal efficiency of SO_2 at different average particle diameters (d_{ps} = 460 μm, C_0 = 500 ppm, U_0 = 20 cm/s, W_{s0} = 1500 g, W_{c0} = 500 g, R.H. = 60% and T = 50°C).

Fig. 13 shows the removal efficiency of sulfur dioxide at different superficial gas velocities. Note that at the superficial gas velocities of 7.5 and 9.5 cm/s, the bed became a fixed bed. It is seen in Fig. 13 that a lower gas velocity had a higher sulfur dioxide removal efficiency due to a higher gas residence time. Similar observation could be made of the calcium conversion shown in Fig. 14. The effect of the superficial gas velocity on total volume of the gas treated until SO_2 outlet concentration reached 150 ppm is shown in Fig. 15. Note that 150 ppm is the standard of the environmental protection regulations in our country. Total volume of the gas treated, V_t, was equal to (gas volumetric flow rate) × (operating time until outlet SO_2 concentration reached 150 ppm). As shown in this figure, it increased initially, reached a maximum, and then decreased with increasing gas velocity. This was due to two counteracting factors. As the gas velocity increased, SO_2 removal efficiency

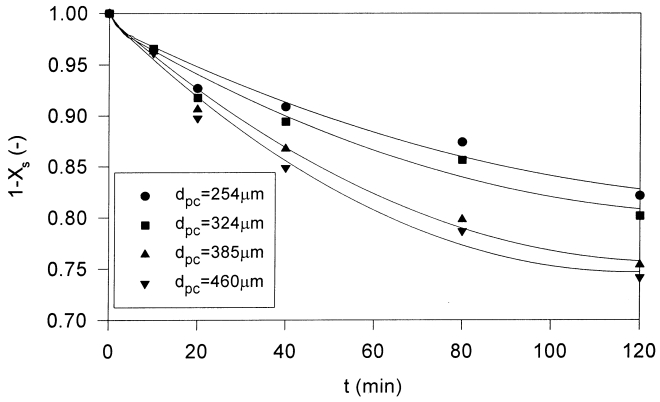

Fig. 11. Conversion of sorbent in the cyclone at different average particle diameters (d_{ps} = 460 μm, C_0 = 500 ppm, U_0 = 20 cm/s, W_{s0} = 1500 g, W_{c0} = 500 g, R.H. = 60% and T = 50°C).

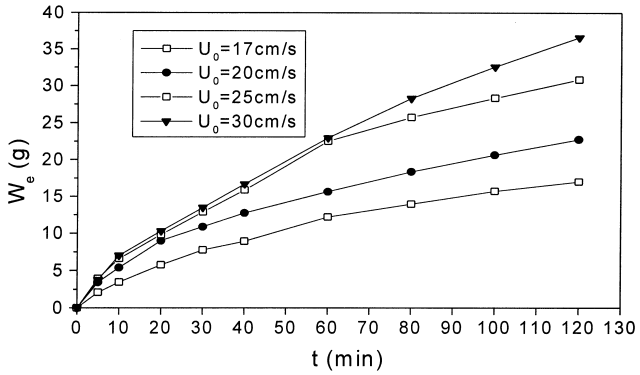

Fig. 12. Cumulative weight of solid elutriated at different superficial gas velocities ($d_{ps} = 460\,\mu m$, $d_{pc} = 385\,\mu m$, $C_0 = 500\,ppm$, $W_{s0} = 1500\,g$, $W_{c0} = 500\,g$, R.H. = 60% and $T = 50^{\circ}C$).

decreased (Fig. 13). However, the volumetric gas flow rate increased with increasing gas velocity. As a result, total volume of the gas treated had a maximum value.

3.5. The attrition model

Arena et al. [14] and Blinichev et al. [15] defined the attrition rate as

$$R_t = -\frac{dW}{dt} = K_a W \tag{2}$$

where W is the weight of the solid in the bed (kg) and K_a the overall attrition rate constant (1/s).

However, Lee et al. [4] observed that the weight of the solid in a fluidized bed would approach a constant value, so they modified Eq. (2)

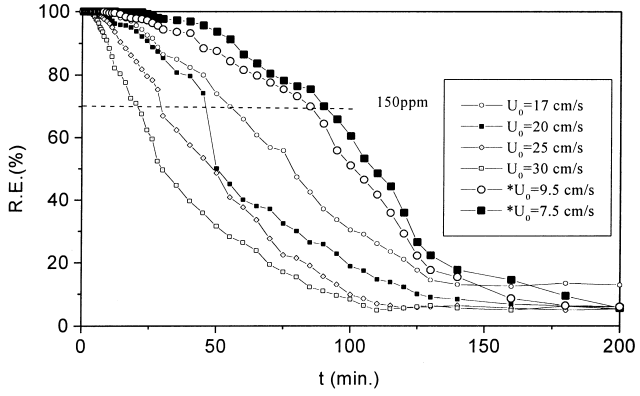

Fig. 13. Removal efficiency of sulfur dioxide at different superficial gas velocities ($d_{ps} = 460\,\mu m$, $d_{pc} = 385\,\mu m$, $C_0 = 500\,ppm$, $W_{s0} = 1500\,g$, $W_{c0} = 500\,g$, R.H. = 60% and $T = 50^{\circ}C$) (* fixed bed).

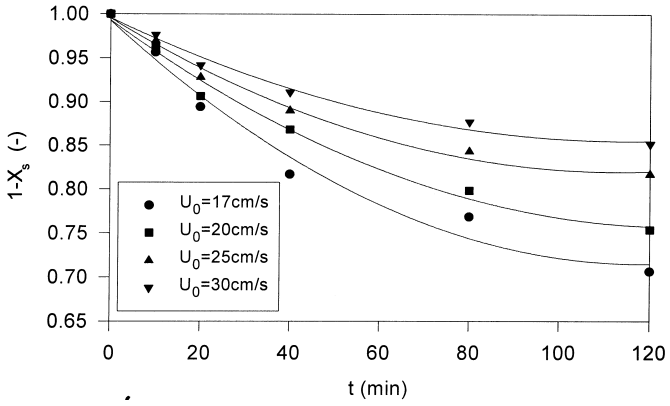

Fig. 14. Conversion of sorbent in the cyclone at different superficial gas velocities ($d_{ps} = 460\,\mu m$, $d_{pc} = 385\,\mu m$, $C_0 = 500\,ppm$, $W_{s0} = 1500\,g$, $W_{c0} = 500\,g$, R.H. = 60% and $T = 50^{\circ}C$).

$$\frac{dW}{dt} = -K_a(W - W_{min}) \tag{3}$$

where W_{min} is the minimum weight of the parent solid in a bed (kg).

Since it was observed in this study that the particle size of the silica sand did not change during the experiments, W_{min} was equal to the initial weight of the silica sand in the fluidized bed, W_{s0}.

According to our experimental results, the attrition rate was strongly influenced by the conversion of the sorbent. Therefore, we assumed the overall attrition rate constant as follows:

$$K_a = k_a(1 - X_s) \tag{4}$$

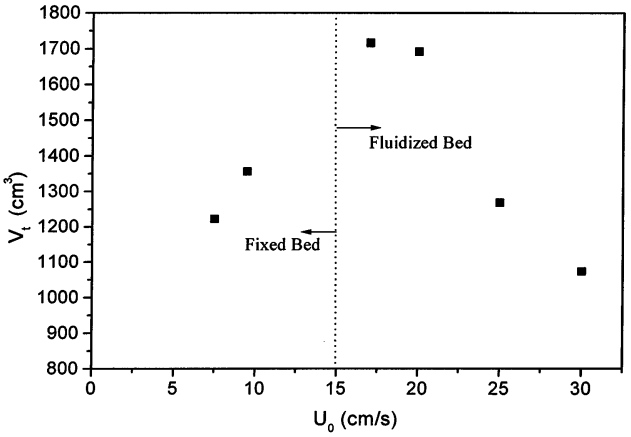

Fig. 15. Total volume of gas treated at different superficial gas velocities ($d_{ps} = 460\,\mu m$, $d_{pc} = 385\,\mu m$, $C_0 = 500\,ppm$, $W_{s0} = 1500\,g$, $W_{c0} = 500\,g$, R.H. = 60% and $T = 50^{\circ}C$).

where X_s is the conversion of the sorbent in the cyclone and k_a the attrition rate constant (1/s). Subsitituting Eq. (4) into Eq. (3), we obtained the following equation:

$$R_t = -\frac{dW}{dt} = k_a(1 - X_s)(W - W_{s0}) \tag{5}$$

Intergration of Eq. (5) gave rise to

$$\ln\frac{W - W_{s0}}{W_0 - W_{s0}} = -k_a\int_0^t (1 - X_s)\,dt \tag{6}$$

Using the initial condition $W_0 = W_{s0} + W_{c0}$, Eq. (6) became

$$W = W_{s0} + W_{c0}\exp\left(-k_a\int_0^t (1 - X_s)\,dt\right) \tag{7}$$

where W_{c0} is the initial weight of the sorbent particles in the fluidized bed.

Cumulative weight of the elutriated solid could then be obtained by

$$W_e = W_0 - W = W_{c0}\left[1 - \exp\left(-k_a\int_0^t (1 - X_s)\,dt\right)\right] \tag{8}$$

Using the experimental results obtained in this study, the value of k_a could be evaluated by Eq. (8). Fig. 16 showed that k_a was constant during a typical experimental run, i.e. it was independent of the sorbent conversion. The average value of k_a in Fig. 16 was $9 \times 10^{-6} \pm 1 \times 10^{-6}$ (1/s) in the 20–120 min range. A plot of k_a versus U_0/d_{pc} was shown in Fig. 17. As shown in this figure, a linear relationship existed between k_a and (U_0/d_{pc}). Therefore,

$$k_a = 1.63 \times 10^{-2}\left(\frac{U_0}{d_{pc}}\right) \tag{9}$$

where U_0 is the superficial gas velocity (m/s) and d_{pc} the average particle diameter of sorbent (m).

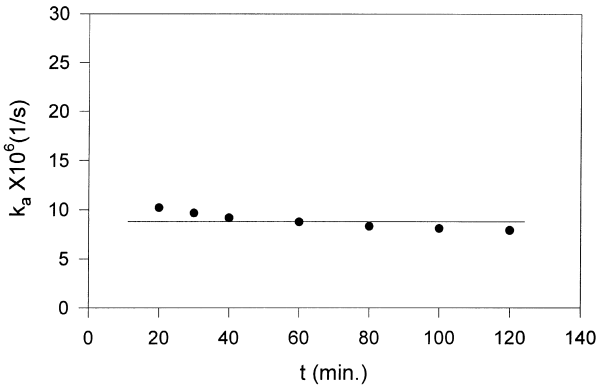

Fig. 16. k_a vs. time ($d_{ps} = 460\,\mu m$, $d_{pc} = 385\,\mu m$, $C_0 = 500$ ppm, $U_0 = 17$ cm/s, $W_{s0} = 1500$ g, $W_{c0} = 500$ g, R.H. = 60% and $T = 50^\circ$C).

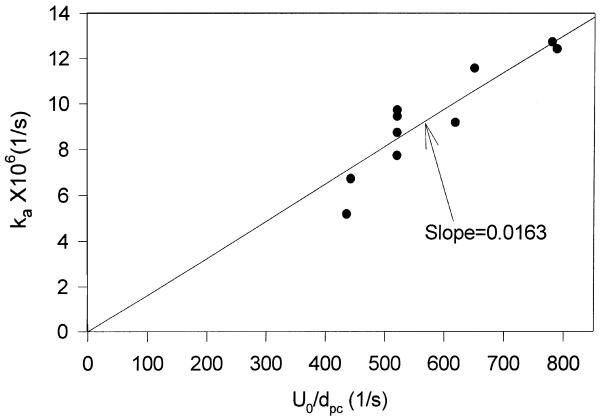

Fig. 17. The relationship between k_a and U_0/d_{pc}.

Eqs. (8) and (9) could then be used to predict the weight of the elutriation. Figs. 18 and 19 compared the experimental data of the weight of the elutriation with those predicted by the proposed model and Lee's model [4]. It should be noted that Lee's model did not consider the effect of the sulfation reaction on the attrition. Furthermore, K_a in Lee's model

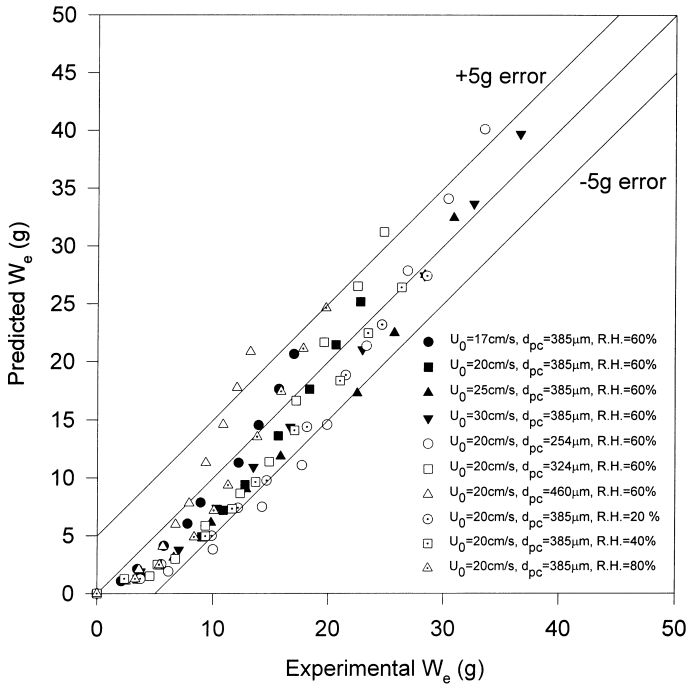

Fig. 18. Predicted weight of the elutriation by this work vs. experimental data ($C_0 = 500$ ppm, $d_{ps} = 460$ μm, $W_{s0} = 1500$ g, $W_{c0} = 500$ g and $T = 50$°C).

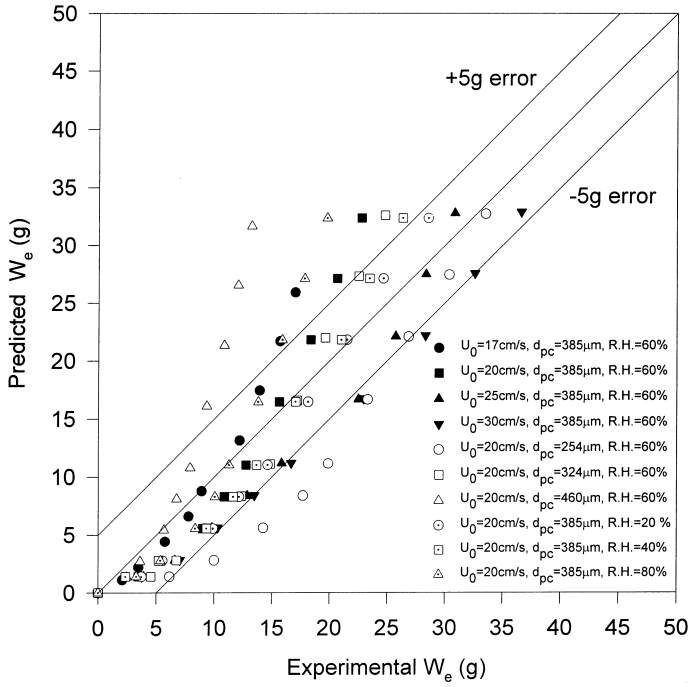

Fig. 19. Predicted weight of the elutriation by Lee et al. [4] vs. experimental data ($C_0 = 500$ ppm, $d_{ps} = 460$ μm, $W_{s0} = 1500$ g, $W_{c0} = 500$ g and $T = 50°$C).

was expressed in an Arrhenius form

$$K_a = K_0 \exp\left(-\frac{E_a RTC_s}{PM_w U_0(U_0 - U_{mf})}\right) \tag{10}$$

where K_0 is the frequency factor in an Arrhenius form, E_a the attrition activation energy (kJ/kg), R the gas constant (kJ/kg mol K), T the temperature (K), C_s the critical weight of solids in a bed (kg/m^3), P the absolute pressure of gas (kg/m s^2), M_w the molecular weight of gas (kg/kg mol) and U_{mf} the minimum fluidization velocity (m/s).

The values of K_0 and E_a calculated from our experimental data were 9.48×10^{-6} and 4.69×10^{-4} (kJ/kg), respectively. It was seen in Figs. 18 and 19 that our model was far better than Lee's model, especially at high sorbent conversions. It should be noted that initially the shape of the sorbent particles was irregular, thus the attrition rates obtained in the experiments initially (at low values of W_e) were higher than the predicted values.

4. Conclusions

Sulfation and attrition of the calcium sorbent in a fluidized bed were investigated in this study. It was found that the effects of the bed temperature ranging from 40 to 65°C on the

removal efficiency of sulfur dioxide, sorbent conversion and attrition were negligible. A higher relative humidity of the gas resulted in a higher sulfur dioxide removal efficiency and a higher calcium conversion. However, the attrition was lower. In addition, a smaller size of the calcium sorbent had a higher sulfur dioxide removal efficiency and attrition, but the calcium conversion was lower. Furthermore, as the superficial gas velocity was increased, the sulfur dioxide removal efficiency and calcium conversion decreased, but the attrition increased. Finally, an attrition model taking into account the effect of the sulfation reaction on the attrition was developed. This model could predict the weight of the elutriation satisfactorily.

Acknowledgements

This study was supported by National Science Council of Republic of China through grant NSC 88-2214-E-007-004.

References

[1] D. Kunii, O. Levenspiel, Fluidization Engineering, 2nd Edition, Butterworth Heinemann Publishing, USA, 1991, p. 1.
[2] Y.C. Ray, T.S. Jiang, C.Y. Wen, Powder Technol. 49 (1987) 193.
[3] W.G. Vaux, D.L. Keairns, in: J.R. Grace, J. M. Matsen (Eds.), Fluidization, Plenum Press, NY, 1980, p. 437.
[4] S.K. Lee, X. Jiang, T.C. Keener, S.J. Khang, Ind. Eng. Chem. Res. 32 (1993) 2758.
[5] A.D. Bernedetto, P. Salatino, Powder Technol. 95 (1998) 119.
[6] H. Kono, AIChE Symp. Ser. 77 (205) (1981) 96.
[7] C.S. Ho, S.M. Shih, J. Chin. IChE 24 (4) (1993) 187.
[8] M. Colakyan, O. Levenspiel, Powder Technol. 38 (1984) 223.
[9] J.L. Cook, S.J. Khang, S.K. Lee, T.C. Keener, Powder Technol. 89 (1996) 1.
[10] J. Klingspor, H.T. Karlsson, I. Bjerle, Chem. Eng. Commun. 22 (1983) 81.
[11] C. Jorgensen, J.C.S. Chang, Environ. Prog. 6 (2) (1987) 26.
[12] D. Merrick, J. Highley, AIChE Symp. Ser. 70 (137) (1974) 366.
[13] L. Lin, J.T. Sears, C.Y. Wen, Powder Technol. 27 (11) (1980) 105.
[14] U. Arena, M. D'amore, L. Massimilla, AIChE J. 29 (1) (1983) 40.
[15] V.N. Blinichev, V.V. Strel'tsov, E.S. Lebedeva, Int. J. Chem. Eng. 8 (4) (1968) 615.